Application of kinetic, isothermal and thermodynamic models in the biosorption of Cd(II), Pb(II) and Zn(II) from solutions onto Melon (*Citrillus lanatus*) seed husk

Adesola Babarinde* and Grace Omisore

Department of Chemical Sciences, Olabisi Onabanjo University, Ago-Iwoye, Ogun State, Nigeria

Abstract

The feasibility of employing melon seed husk for the biosorption of Cd(II), Pb(II), and Zn(II) from aqueous solution has been investigated under different physicochemical parameters. The extent of biosorption of each metal ion was found to be dependent on the solution pH, contact time, biosorbent dose, initial metal ion concentration, and temperature. The study on the FTIR showed the presence of ionizable groups and lone pairs that could participate in the binding of metal ions in solution. Biosorption mechanisms were also investigated using the pseudo-first-order, pseudo-second-order, Elovich, and Intraparticle diffusion kinetic models. The kinetic results showed that the biosorption of Cd(II), Pb(II), and Zn(II) onto melon seed husk best followed pseudo-second-order kinetics. The study on the effect of dosage showed that the dosage of the biomass significantly affected the uptake of the metal ions from solution. The experimental equilibrium biosorption data were analyzed with four widely known Isotherms parameters: Langmuir, Freundlich, Temkin, and Dubinin-Radushkevich (D-R) isotherm models. The Freundlich isotherm model gave the best fit with the highest correlation coefficient, R^2. Thermodynamically, each process was found to be endothermic while the order of spontaneity and the order of disorder was found to be Zn(II)> Cd(II)> Pb(II).

1. Introduction

Heavy metals are recognized as long-term hazardous contaminants because of their high toxicity, accumulation and retention in human body. Cd(II), Pb(II), and Zn(II) are toxic metals responsible for causing kidney disorder, renal disorder, high blood pressure, and destruction of red blood cells [1]. Major sources of these toxic metals in the environment are electroplating, pigment industries, plastic and metal finishing industries. The conventional methods for the removal of heavy metals from industrial effluents include chemical precipitation [2], ion exchange [3], electrochemical precipitation [4], membrane separation [5], and adsorption [6-8]. All these methods are, in this case, either economically unfavourable or technically complicated and thus used only in special cases. Each of these methods has some limitations in practice. The problems with the aforementioned methods make it necessary to develop easily available, inexpensive, eco-friendly, and equally effective alternatives for water and wastewater treatment. Biosorption of heavy metals by agricultural waste materials, which are produced in large quantities as a solid waste, is one of these alternative treatment methods [9-12].

Melon seed husk (MSH), an agricultural waste, was used as biosorbent for Cd(II), Pb(II), and Zn(II) from aqueous solutions. Melon (*Citrillus lanatus*) belongs to the family of Cucurbitaceae. It is a wild melon similar in appearance to the water melon. It originates from the western Kalahari region of Namibia and Botswana. In this region, there are two major types, one with small bitter fruits that are mainly used for their seeds and the other has fruits that are mainly used as source of water during periods of drought. The flesh is inedible but the seeds are a valuable food source in Africa [13]. The seeds are the true delicacy of this melon. The high oil and protein content can make an excellent dietary supplement. The seeds are often shelled and eaten as snacks or processed into common cooking practices. The oil gotten from the seed ensures a good supply of polysaturated fatty acids that has protective effect against coronary heart disease (CHD) and improves insulin sensitivity. However, there is known use of the melon seed husk, hence it is turns out to be an environmental nuisance. This reason prompted this study to determine the possibility of utilizing such an agricultural waste for bioremediation in view of the large quantities of melon produced yearly worldwide.

2. Material and Methods

2.1. Biomass preparation

Melon (*Citrullus lanatus*) seeds were gotten from a market in Ago-Iwoye, Ogun State, Nigeria. The light brown husk covering the whitish seed were removed manually. The husks were collected inside a nylon bag. The husks were extensively washed with distilled water to remove dirt and other particulate matter that might interact with sorbed metal ions. It was then air dried immediately and kept dry till time of usage.

2.2. Preparation of solution

All chemicals used in this study were of analytical reagent grade and were used without further purification. Standard solutions of Cd(II), Pb(II), and Zn(II) used for this study were prepared from $Cd(NO_3)_2.4H_2O$, $Pb(NO_3)_2$, $Zn(NO_3)_2.6H_2O$, respectively. The working solutions with different concentrations of the metal ions were prepared by appropriate dilutions of the stock solution immediately prior to their use with distilled water. The initial pH of the solution was adjusted accordingly with a pH meter. Each boiling tube used for the biosorption was suspended in a thermostated water bath. The concentration before and after biosorption of each metal ion was determined using a Perkin-Elmer analyst 700 flame Atomic Absorption Spectrophotometer (AAS) with deuterium background corrector. Fourier Transform Infrared (FTIR) spectra of dried unloaded biomass and metal loaded biomass are recorded at 400-4000cm^{-1}, using a Shimadzu FTIR model 8400 S spectrophotometer.

2.3. Batch biosorption study

The biosorption study was determined by batch experiments by contacting 0.5g of the Melon (*Citrillus lanatus*) seed husk with 25ml of each metal ion solution under different conditions for a period of time in a glass tube. The biosorption studies were conducted at 25°C using thermostated water bath to determine the effect of pH, contact time, biosorbent dosage, initial metal ion concentration and temperature on the biosorption of each metal ion. The residual metal ions were analyzed using AAS. The amount of metal ion biosorbed from solution was determined by difference and the mean value calculated.

2.4. Statistical Analyses

The curve fittings of the data obtained were performed using Microcal Origin 6.0 software.

3. Results and Discussion

3.1. Physical characterization of MSH

The functional groups present on the surface of melon seed husk would give insight to the feasibility of biosorption of metal ions by the biomass. These groups would form active sites for sorption on the material surface. The FT-IR spectra of dried unloaded, Cd-loaded, Pb-loaded and Zn-loaded melon seed husk were taken to obtain information on the nature of possible interactions between the functional groups of melon seed husk and the metal ions as presented in Figure 1. The FT-IR spectra pattern of the biomass showed distinct and sharp absorptions indicative of the existence of the functional groups such as -OH, C-O, and C≡N groups as shown in Figure 1. These bands are due

to the functional groups of melon seed husk that participate in the biosorption of Cd(II), Pb(II) and Zn(II). On comparison, there are clear band shifts and decrease in intensity of bands. The FT-IR spectra of the melon seed husk biomass indicated slight changes in the absorption peak frequencies due to the fact that the binding of the metal ions causes change in absorption frequencies. These shifts in absorbance observed implies that there were metal binding processes taking place on the active sites of the biomass. Analysis of the FT-IR spectra showed the presence of ionizable functional groups which are able to interact with cations [14-18]. This implies that these functional groups would serve in the removal of positively charged ions from solution.

3.2. Effect of solution pH on metal ion biosorption

The pH of the solution is an important parameter governing the uptake of heavy metals by biosorption process as it affects both metal species in solution, the surface properties of biosorbents in terms of dissociation of binding sites and surface charge [19]. The pH usually plays an important role in the biosorption of the metal ions [20]. The net charge of the sorbate and that of the sorbent are dependent on the pH of the solution. At low pH, the metal ion uptake is inhibited by net positive charge on the sorbent and the competition between the metal ions and the hydrogen ions in solution. As the pH increases, the negative charge density on biomass increases as a result of deprotonation of the metal binding sites on the biomass, consequently, the biosorption of the metal ions increases. Figure 2 shows the variation of the metal ions biosorbed on melon seed husk at various pH values. For the three metal ions, the biosorption increased as the pH increased from pH 1 to 6. The increase observed in the biosorption with increase in pH implies that ion exchange process was involved.

The reaction is a reversible one with an equilibrium being made between the metal ion (represented as M^{x+}) and the biosorbent with lone pair of electron (represented as Ä). The two phases are schematically shown below for a divalent metal ion in solution:

$$\ddot{A} + M^{2+} \rightleftharpoons A\text{-}M \qquad (1)$$

3.3. Biosorption kinetics

Figure 3 illustrates the dynamic biosorption process of the three metal ions on melon seed husk. It is observed that the biosorptive quantities of the three metal ions on the melon seed husk increased with increasing contact time. In each case, biphasic kinetics are observed: an initial rapid stage (fast phase) where biosorption is fast and contributes to equilibrium uptake and a second stage (slow phase) whose contribution to the metal ion biosorbed is relatively smaller. The fast phase is the instantaneous biosorption stage, it is assumed to be caused by external biosorption of metal ion to the biomass surface. The second phase is a gradual biosorption stage, whose diffusion rate is controlled. Finally, the biosorption sites are used up, the uptake of the metal ion reached equilibrium. This phase mechanism has been suggested to involve two diffusion processes, external and internal, respectively [21]. The biosorption of each of the metal ions eventually achieves equilibrium, although

their rates of uptake and times of reaching equilibrium are different. This might be due to the differences in hydrated ionic sizes of the metal ions [22].

In order to establish the mechanism of the biosorption of Cd(II), Pb(II), and Zn(II) unto melon seed husk, four kinetic models were applied to the biosorption process. These are the pseudo-first-order, pseudo-second-order, Elovich, and Intraparticle model equations. One of such models is the Lagergren pseudo-first-order model which considers that the rate of occupation of the biosorption site is proportional to the number of the unoccupied sites [18].

$$rate = -\frac{d[A]}{dt} = k\,[A]^n \tag{2}$$

Which can also be written as

$$\frac{d}{dt}q_t = k_1(q_e - q_t) \tag{3}$$

Integrating between the limits $q_t = 0$ at $t = 0$ and $q_t = q_t$ at $t = t$, we obtain

$$\log\left[\frac{q_e}{(q_e - q_t)}\right] = \frac{k_1}{2.303}t \tag{4}$$

This can be rearranged to obtain a linear form

$$\log(q_e - q_t) = \log q_e - \frac{k_1}{2.303}t \tag{5}$$

where k_1 is the Lagergren rate constant of the biosorption (min^{-1}); q_e and q_t are the amounts of metal ions sorbed (mgg^{-1}) at equilibrium and at time t, respectively. The plot of $\log(q_e - q_t)$ versus t for the biosorption of metal ions on melon seed husk at initial concentration of 100 mg L^{-1} should give a straight line for a process that follows first-order kinetic model as represented in Figure 4. The kinetic parameters are presented in Table 1.

The data was equally subjected to the pseudo-second-order kinetic model. The pseudo-second-order kinetic model is represented as

$$\frac{d}{d_t}q_t = k_2(q_e - q_t)^2 \tag{6}$$

On integrating between boundary conditions, we have

$$\frac{1}{q_e - q_t} = \frac{1}{q_e} + k_2 t \tag{7}$$

On rearrangement, we have

$$\frac{t}{q_t} = \frac{1}{k_2 q_e^2} + \frac{1}{q_e}t \tag{8}$$

Where k_2 is the equilibrium rate constant of pseudo-second-order biosorption process (g mg^{-1} min^{-1}). However, plots of t versus t/q_t showed good fitness of experimental data with the pseudo-second-order kinetic model as presented in Fig. 5. The kinetic parameters are presented in Table 1.

The data were equally subjected to the Elovich kinetic model given by

$$q_t = A + B \ln t \tag{9}$$

Where q_e is the amount (mgL^{-1}) of metal ion biosorbed after a given time t. The Elovich kinetic plot is presented in Figure 6 while the kinetic parameters are presented in Table 1.

The intraparticle diffusion equation was also applied to the kinetic data, it is given as

$$R = K_s t^b \tag{10}$$

The intraparticle diffusion equation has been used to indicate the behaviour of intraparticule diffusion as the rate limiting step in the biosorption process. R is the percent metal ions biosorbed, K_s is the intraparticle diffusion constant, t is the contact time, while b is the gradient of the linear plot. In the linear form, equation (10) turns to

$$\log R = b \log t + \log K_s \tag{11}$$

The Intraparticle kinetic plot is presented in Figure 7 while the kinetic parameters are presented in Table 2. For the four kinetic model tested, the kinetic parameters are presented in Table 1. On comparison of the values of R^2 for the experimental points, the correlation coeffficents obtained were found to be highest for the pseudo-second-order kinetics and were found to be in excess of 0.998, 0.999 and 0.996 for Cd(II), Pb(II), and Zn(II), respectively. The pseudo-second-order kinetic model is therefore, the best kinetic model to predict the dynamic biosorption of Cd(II), Pb(II), and Zn(II) on melon seed husk. The result shows that the rate of biosorption of the metal ions is of the order Pb(II) >Zn(II) >Cd(II). The biosorption capacity is in the order Pb(II) > Cd(II) > Zn(II). The differences observed in the rate of biosorption as well as in the biosorption capacity may be accounted for in terms of the differences in ionic charges, chemical affinity, ion exchange capacity and the hydrated ionic sizes of the ions in solution [22].

3.4. Effect of biomass dosage on biosorption

The effect of biomass dosage on biosorption efficiency is reported in Figure 8. The general trend of increase in the three metal ions biosorbed with increase in biomass dosage indicates an increase in uptake due to more binding sites on the biomass available for biosorption. This is due to the fact that increase in biomass dosage leads to increase in the number of active sites available for biosorption. Hence, the amount of metal ions available for biosorption per gram of biosorbent will be less when the amount of biosorbent is increased. The difference in biosorption capacity q (mgg^{-1}) at the same initial metal ion concentration and contact time may also be attributed to the difference in their chemical affinities and ion exchange capacity, with respect to the chemical functional group on the surface of the biosorbent. This trend has been reported for other biosorbents [23].

3.5. Biosorption Isotherms

An adsorption isotherm represents the equilibrium relationship between the adsorbate concentration in the liquid phase and that on the biosorbent at a given condition. A number of isotherms have been developed to describe equilibrium relationships. In this study, Freundlich, Langmuir, Temkin and Dubinin-Radushkevich (D-R) isotherms were employed to calculate the biosorption capacity.
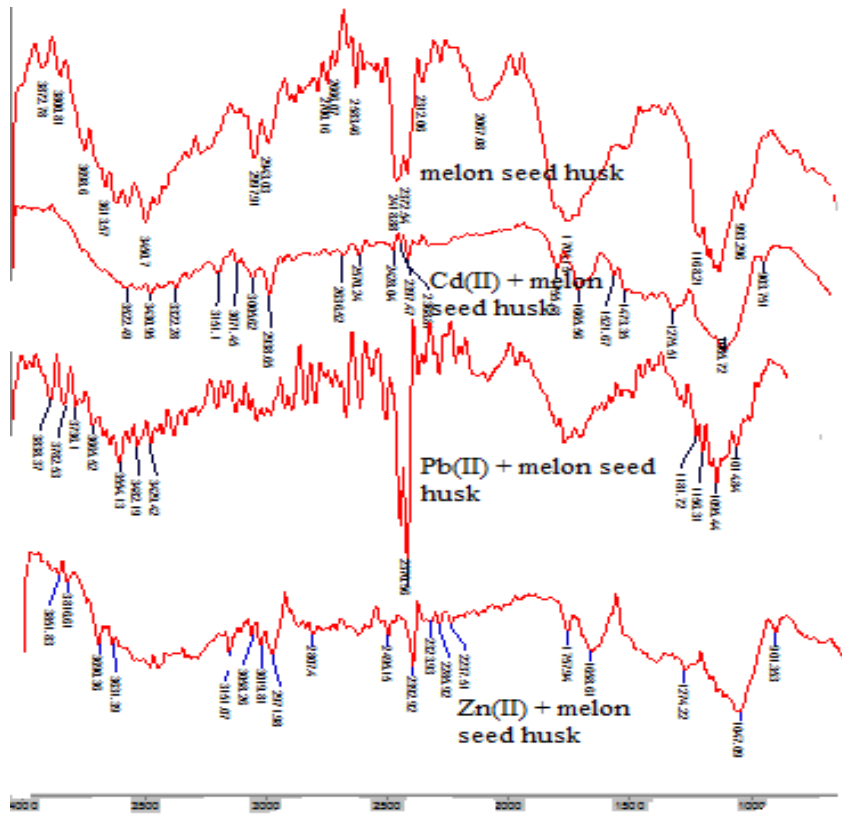
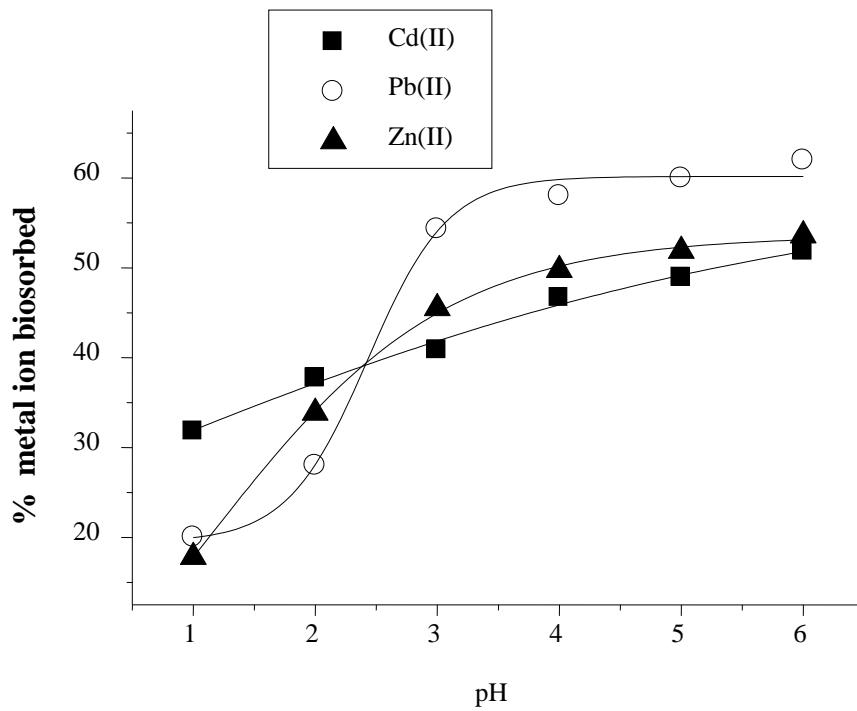**Fig. 1.** FTIR spectra of the free and metal bound MSH at 100 mgL^{-1}

Fig. 2. pH dependence profile for the biosorption of Cd(II), Pb(II), and Zn(II) onto MSH at 100 mgL^{-1}
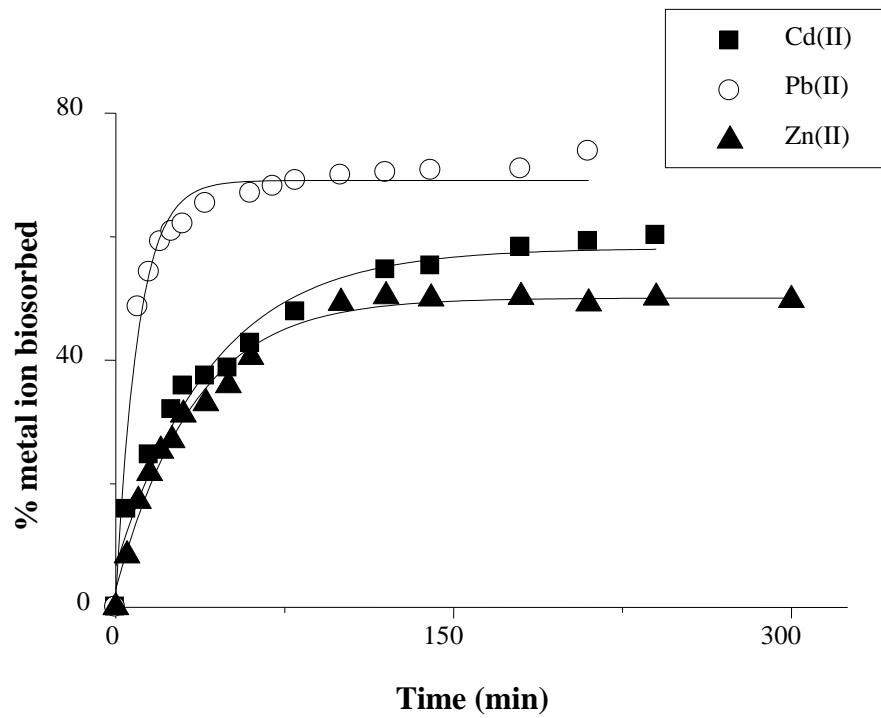
Fig. 3. Time dependence profile for the biosorption of Cd(II), Pb(II), and Zn(II) MSH at 100 mgL^{-1}
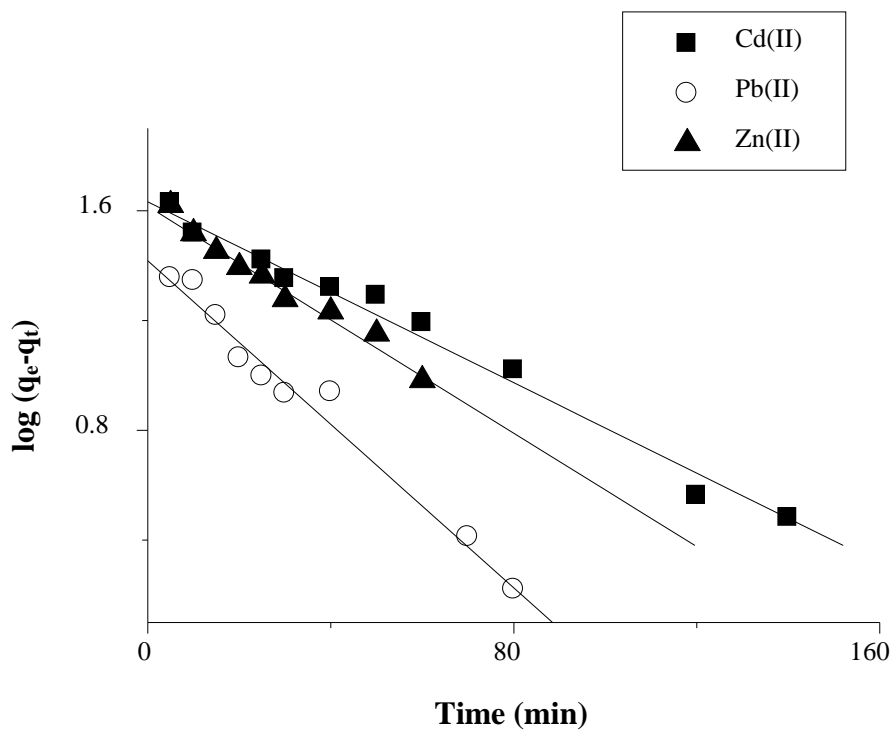

Fig. 4. Pseudo-first-order kinetic plot for the biosorption of Cd(II), Pb(II), and Zn(II) ontoMSH at 100 mgL^{-1}
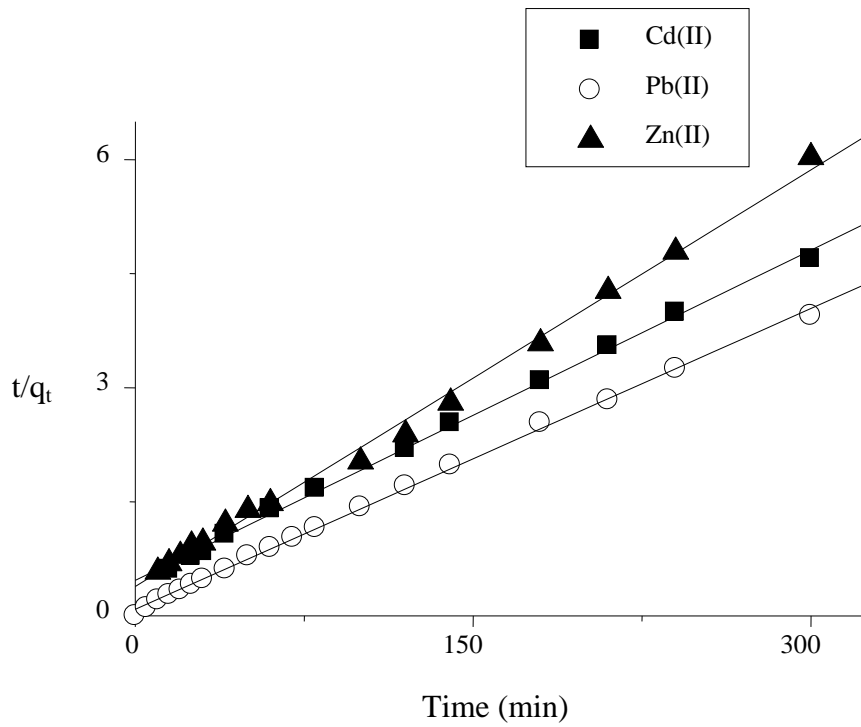
Fig. 5.. Pseudo-second-order kinetic plot for the biosorption of Cd(II), Pb(II), and Zn(II) onto MSH at 100 mgL^{-1}
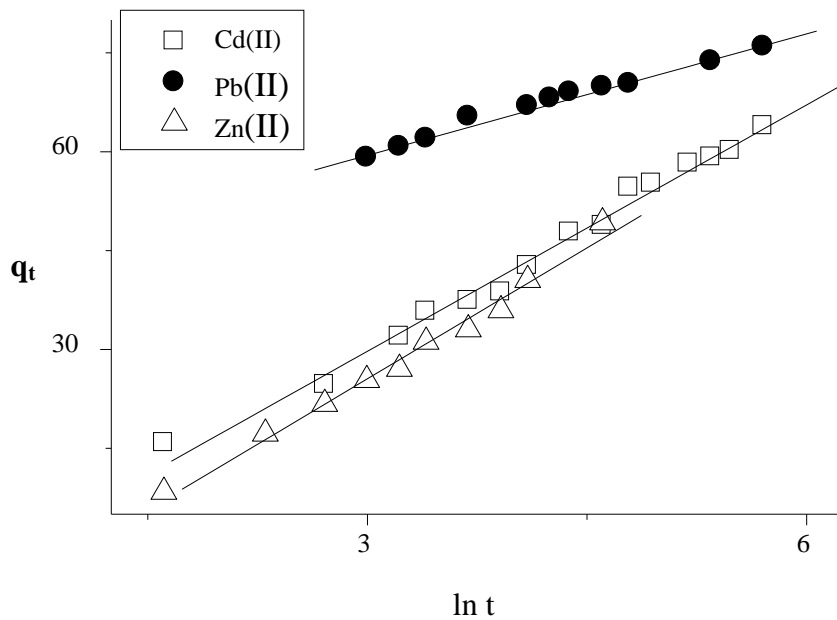

Fig. 6. Elovich plot for the biosorption of Cd(II), Pb(II), and Zn(II) onto MSH at 100 mgL^{-1}
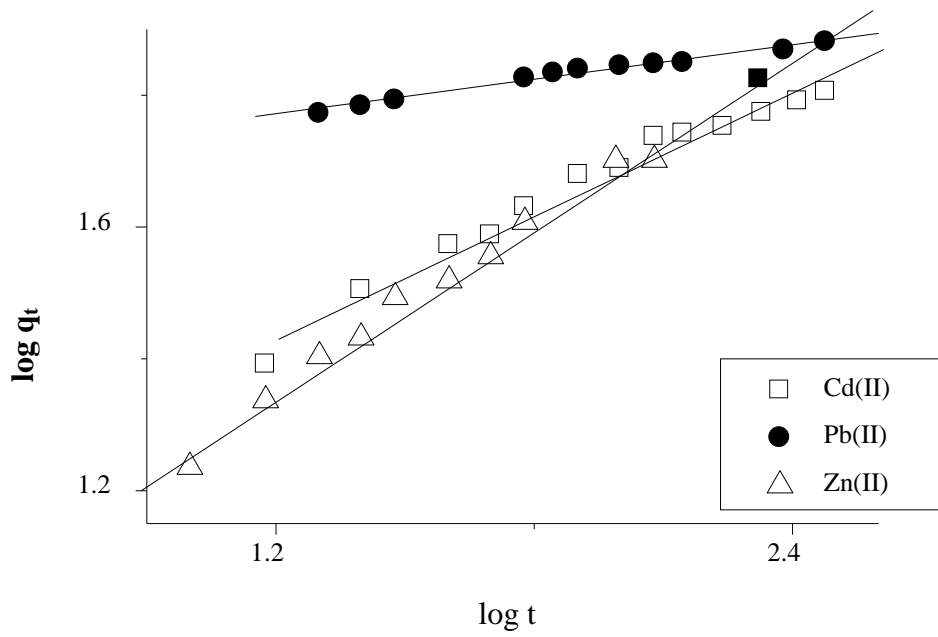
Fig. 7. Intraparticle diffusion kinetic plot for the biosorption of Cd(II), Pb(II), and Zn(II) onto MSH at 100 mgL[-1]
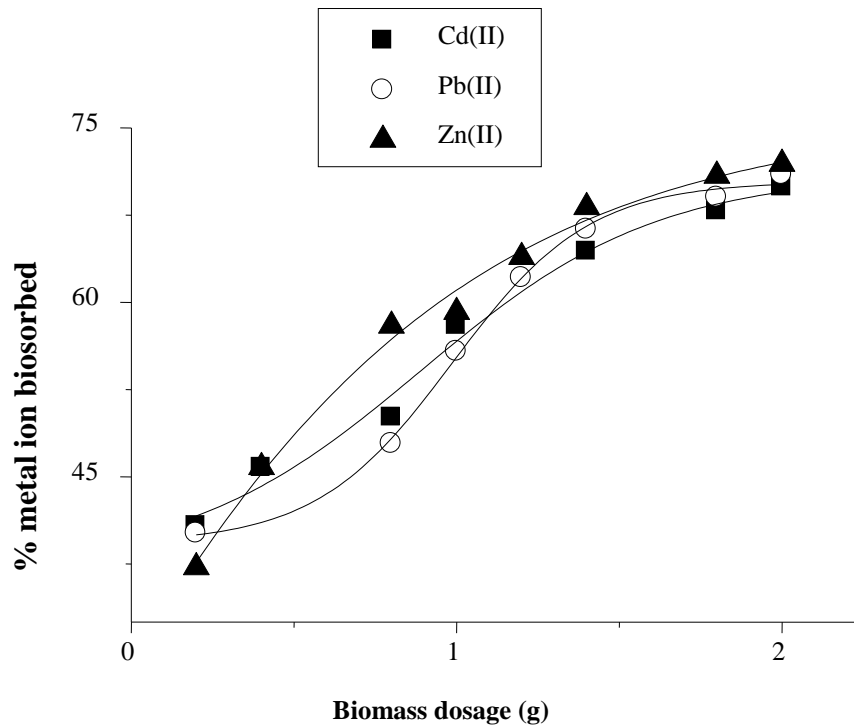
Fig. 8. Effect of biosorbent dose on the biosorption of CdII), Pb(II) and Zn(II) onto MSH at 100 mgL[-1]

Fig. 9. Freundlich isotherm for biosorption of Cd(II), Pb(II) and Zn(II) onto MSH

Fig. 10. Langmuir Isotherm for biosorption of Cd(II), Pb(II) and Zn(II) onto MSH

Fig. 11: Temkin Isotherm for biosorption of Cd(II), Pb(II) and Zn(II) onto MSH

Fig. 12. D-R Isotherm for biosorption of Cd(II), Pb(II) and Zn(II) onto MSH

Fig. 13. Percentage removal Efficiency for the biosorption of Cd(II), Pb(II) and Zn(II) onto MSH

Fig. 14. Thermodynamic plots for the biosorption of Cd(II), Pb(II) and Zn(II) onto MSH at 100 mgL^{-1}

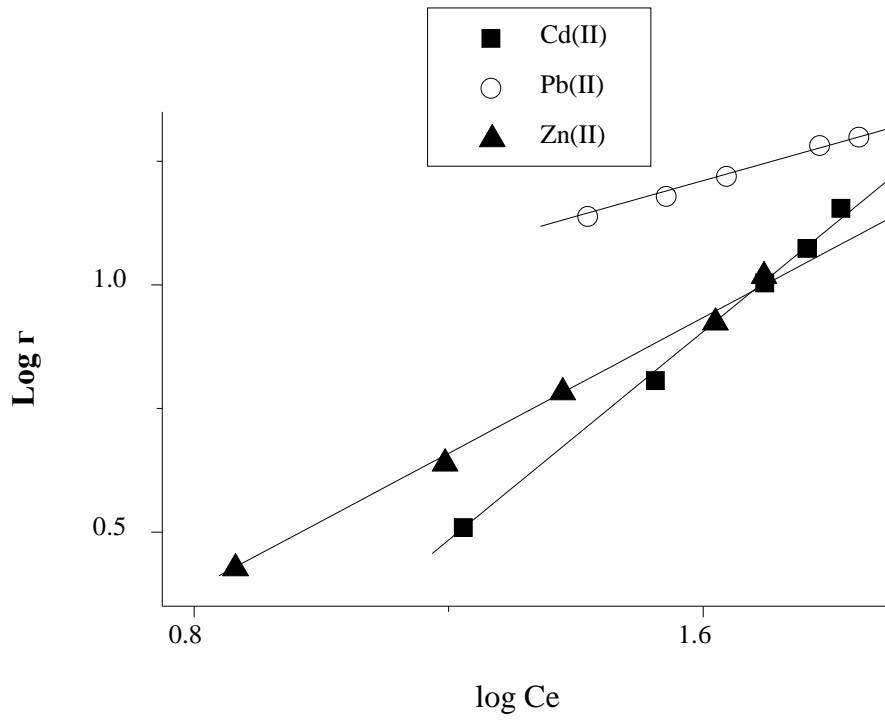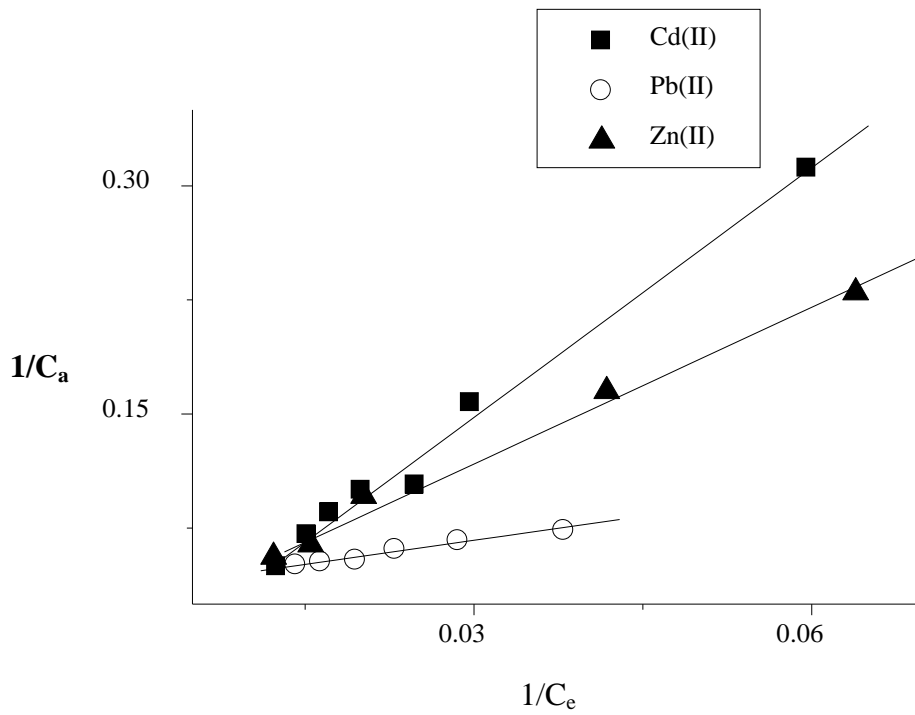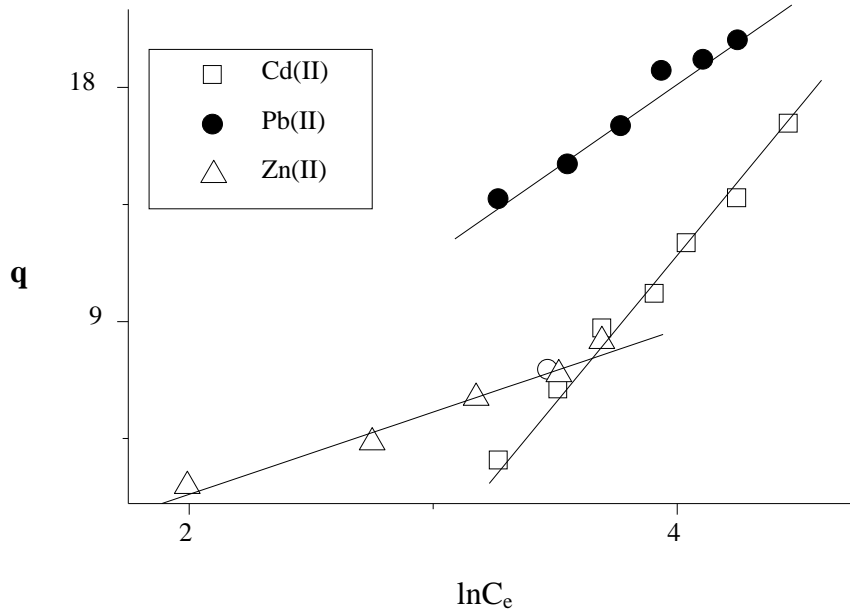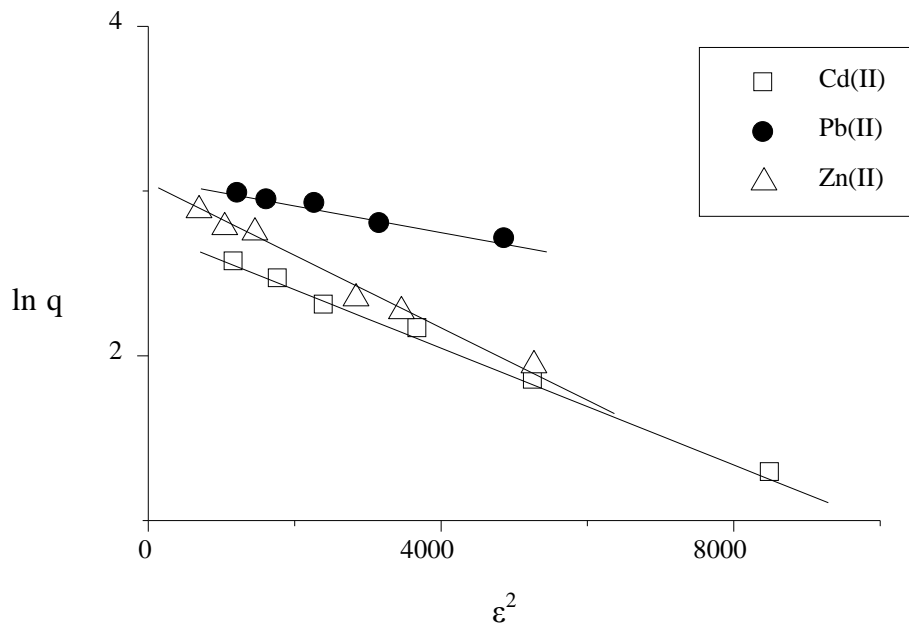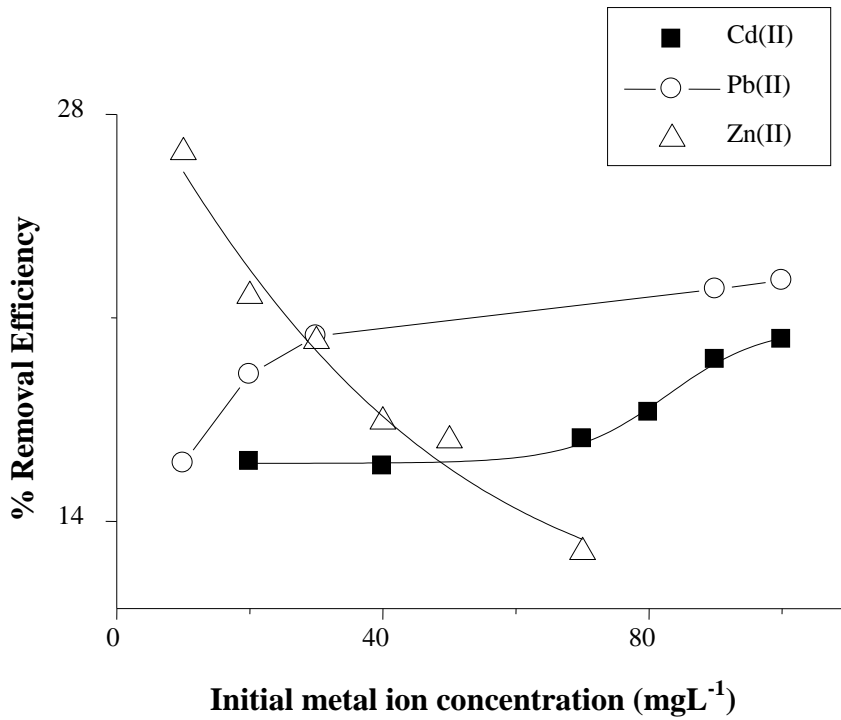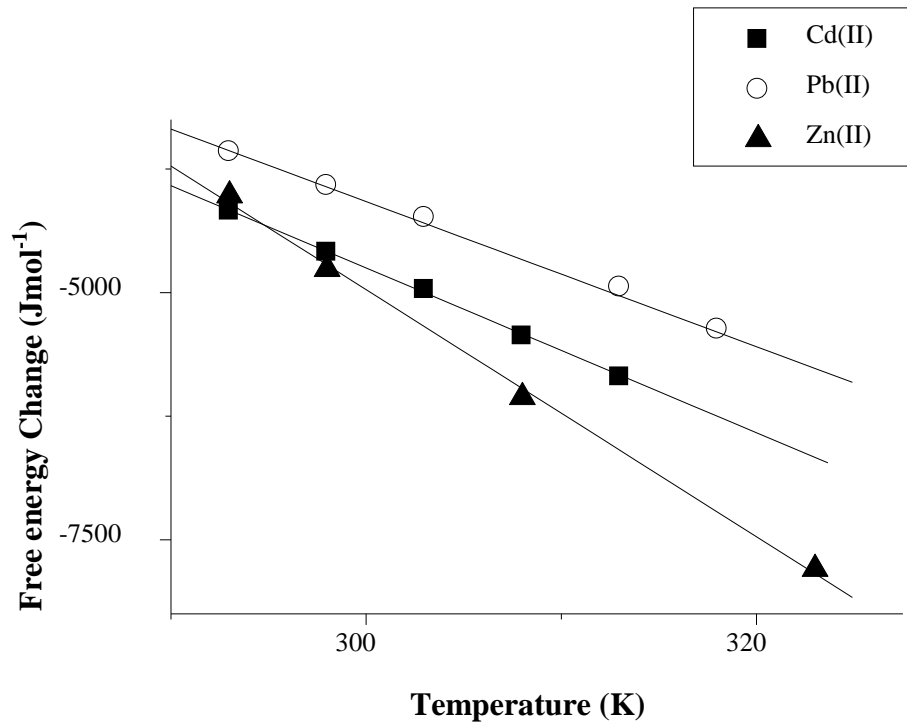**Table 1.** Kinetic parameters for the biosorption of Cd(II), Pb(II) and Zn(II) onto MSH at 100 mgL^{-1}

Kinetic model	Parameters	Cd(II)	Pb(II)	Zn(II)
Pseudo-first-order	$q_{e(mgg^{-1})}$	44.72	26.70	42.37
	$k_{1 (min^{-1})}$	1.9×10^{-2}	3.4×10^{-2}	2.4×10^{-2}
	R^2	0.985	0.978	0.976
Pseudo-second-order	$q_{e, cal(mgg^{-1})}$	69.06	75.82	54.77
	$k_{2(g mg^{-1} min^{-1})}$	4.507×10^{-4}	2.018×10^{-3}	8.626×10^{-4}
	R^2	0.998	0.999	0.996
Elovich	A	-6.93	41.76	-13.71
	B	12.35	6.07	13.12
	R^2	0.988	0.986	0.987
Intraparticle diffusion	$K_{d(mgg^{-1} min^{-½})}$	11.70	45.93	6.81
	B	0.31	0.09	0.43
	R^2	0.974	0.979	0.989

Table 2. Isothermal parameters for the biosorption of Cd(II), Pb(II) and Zn(II) onto MSH at 100 mgL^{-1}

Kinetic model	Parameters	Cd(II)	Pb(II)	Zn(II)
Freundlich	n	0.9302	2.571	1.4389
	$K_{f (mgg^{-1})(Lmg^{-1})^{1/n}}$	0.15	3.81	0.66
	R^2	0.997	0.997	0.9954
Langmuir	$q_{max}(mgg^{-1})$	-66.62	27.58	53.33
	$K_{L(L mg^{-1})}$	-0.0027	0.0362	0.0056
	R^2	0.990	0.975	0.991
Temkin	A	0.05	0.2906	0.2859
	$B(mgg^{-1})$	11.90	6.622	3.195
	R^2	0.9776	0.9737	0.9705
D-R	$q_m (mgg^{-1})$	16.75	21.71	20.80
	$\beta(mol^2 J^{-2})$	1×10^{-4}	8×10^{-5}	2.3×10^{-4}
	$E(Jmol^{-1})$	70.71	79.05	46.62
	R^2	0.9877	0.9711	0.9385

Table 3. Thermodynamic parameters for the biosorption of Cd(II), Pb(II) and Zn(II) onto MSH

Metal ion	ΔH^o (kJmol^{-1})	ΔS^o(JK^{-1}mol^{-1})	R^2	A (kJmol^{-1}) @ (303K)	A(kJmol^{-1}) @ (318K)
Cd(II)	+20.42	+83.93	0.999	22.92	23.00
Pb(II)	+17.28	+71.12	0.998	19.78	19.92
Zn(II)	+32.54	+125.05	0.998	35.08	35.10

The Freundlich Isotherm Model is an empirical equation describing adsorption onto a heterogenous surface. The Freundlich isotherm is expressed as

$$\log \Gamma = \frac{1}{n}\log C_e + \log K_f \qquad (12)$$

Where K_f and n are the Freundlich constants related to the biosorption capacity (mgg^{-1}) and biosorption intensity of the biosorbent, respectively. Figures 9 illustrates the biosorption isotherm of Cd(II), Pb(II) and Zn(II) onto melon (*Citrullus lanatus*) seed husk. The equilibrium biosorption capacity, q_e, increases with increase in metal ions concentration. The isothermal parameters are presented in Table 2.

The Langmuir Isotherm Model was used to describe observed sorption phenomena and suggests that uptake occurs on a homogenous surface by monolayer sorption without interaction between adsorbed molecules. The linear form of the Langmuir equation is expressed as

$$\frac{1}{q_e} = \frac{1}{q_{max}K_L}\frac{1}{C_e} + \frac{1}{q_{max}} \qquad (13)$$

Where C_e is the equilibrium concentration of metal ion (mgL^{-1}), q_e is the amount of metal ion biosorbed per specific amount of biosorbent (mgg^{-1}), q_{max} is the maximum biosorption capacity (mgg^{-1}), and K_L is an equilibrium constant (Lmg^{-1}) related to energy of bisorption which quantitatively reflects the affinity between the biosorbent and the biosorbate. Where q_{max} and K_L can be determined from the linear plot of $1/q_e$ versus $1/C_e$. The shape of the Langmuir isotherm can be used to predict whether a sorption is favourable or unfavourable in a batch biosorption process. The essential features of the isotherm can be expressed in nterms of a dmensionless constant separation factor, R_L, which is defined [24] as

$$R_L = \frac{1}{1+K_L C_i} \qquad (14)$$

Where C_i is the initial concentration (mgL^{-1}) and K_L is the Langmuir equilibrium constant (Lmg^{-1}). The value of the separation factor, R_L, provides vital information about the nature of biosorption. The value of R_L implies the type of Langmuir isotherm to be reversible ($R_L=0$), favourable ($0< R_L<1$), linear ($R_L=1$), or unfavourable ($R_L>1$) [12]. The Langmuir isotherm is presented in Figure 10 while the evaluated constants are given in Table 2.

The Temkin Isotherm model was also used to fit the experimental data. Unlike the Langmuir and Freundlich, the Temkin isotherm takes into account the interactions between biosorbents and metal ions to be biosorbed and it is based on the assumption that the free energy of sorption is a function of the surface coverage [25]. The linear form of the Temkin isotherm is represented as:

$$q = B\ln A + B\ln C_e \qquad (14)$$

Where C_e is concentration of the biosorbate at equilibrium (mgL^{-1}), q_e is the amount of adsorbate adsorbed at equilibrium (mgg^{-1}). RT/b_T = B where T is the temperature (K) and R is the ideal gas constant (8.314Jmol^{-1}K^{-1}) and A and b_T are constants. A plot of q_e versus $\ln C_e$ enables the determination of constants A and b_T. The constant B is related to the heat of adsorbtion and A is the equilibrium binding constant (Lmin^{-1}) corresponding to the maximum binding energy. The Temkin isotherm is presented in Figure 11 while the evaluated constants are given in Table 2.

The Dubinin-Radushkevich (D-R) **isotherm model** was used to estimate the heterogeneity of the surface energies. The D-R isotherm equation is linearly represented as

$$\ln q = \ln q_m - \beta \varepsilon^2 \qquad (15)$$

$$\varepsilon = RTln(1 + \frac{1}{C_e}) \qquad (16)$$

where q_m is the theoretical saturation capacity (molg^{-1}), β is a constant related to the mean free energy of adsorption per mole of the adsorbate (mol^{2}J^{-2}), and ε is the polanyi potential, C_e is the equilibrium concentration of adsorbate in solution (moll^{-1}), R (Jmol^{-1}K^{-1}) is the gas constant and T (K) is the absolute temperature. The D-R constants q_m and β were calculated from the linear plots of $\ln q_e$ versus ε^2 of Figure 12 are presented in Table 2. The constant β gives an idea about the mean free energy E (Jmol^{-1}) of biosorption per molecule of the biosorbate when it is transferred to the surface of the solid from infinity in the solution and can be calculated from the relationship [26]

$$E = \frac{1}{\sqrt{2B}} \qquad (17)$$

if the magnitude of E is between 8 and 16 kJmol^{-1}, the sorption process is supposed to proceed via chemisorption but if E is less than 8 kJmol^{-1}, the sorption process is of physical nature [26].

The isothermal parameters for the four isotherm applied are presented in Table 3. On comparison of the values of R^2 for the experimental points, the correlation coeffficents obtained were found to be highest for the Freundlich isotherm and were found to be in excess of 0.997, 0.997 and 0.995 for Cd(II), Pb(II), and Zn(II) , respectively. The Freundlich isotherm is therefore, the best isotherm to predict the dynamic biosorption of Cd(II), Pb(II), and Zn(II) on melon seed husk. The value of E is less than 1 kJmol^{-1} for each metal ion implying that each metal biosorption process proceeded via physicosorption.

3.6. Biosorption Efficiency

The biosorption efficiency (E) for each metal ion was calculated as

$$E = 100\left(\frac{C_i - C_e}{C_i}\right) \qquad (14)$$

Where C_i and C_e are the initial and the equilibrium metal ion concentrations (mgL^{-1}), respectively. The result of the study on the effect of initial metal ion concentration on biosorption efficiency is shown in Figure 13. The plots show that the biosorption efficiency of the biomass reduces with increase in the initial metal ion concentration for Zn(II) which might be due to increase in effective collision between the metal ions and the active sites in the biosorbent having more ions than at lower concentration. On the other hand, the biosorption efficiency increased with the increase in initial metal ion concentration for Cd(II) and Pb(II) which might be due to increase in the number of active sites available for biosorption as the dosage increases.

3.7. Biosorption Thermodynamics

The biosorption of metal ions may involve chemical bond formation and ion exchange since temperature is a major parameter affecting them. The

variation of temperature affects the biosorption of metal ions onto solid surfaces of biomass since the biosorption process is a reversible one. The nature of each side of the equilibrium determines the effect temperature has on the position of equilibrium. The side that is endothermic is favoured by increase in temperature while the contrary holds for the exothermic side. The corresponding free energy change was calculated from the relation [17, 27].

$$\Delta G^\circ = -RT \ln K_c$$

(15)

Where T (K) is the absolute temperature. The equilibrium constant (K_c) was calculated from the following relationship.

$$K_c = \frac{C_{ad}}{C_e}$$

(16)

Where C_e and C_{ad} are the equilibrium concentrations of metal ions (mgL^{-1}) in solution and on biosorbent , respectively. Consequently, the thermodynamic behaviour of the biosorption of Cd(II), Pb(II) and Zn(II) onto melon seed husk was evaluated through the change in free energy (ΔG°), enthalpy (ΔH°) and entropy (ΔS°). The thermodynamic parameters like enthalpy and entropy were obtained using van't Hoff equation [14, 28]. The change in free energy is related to other thermodynamic properties as

$$\Delta G^\circ = \Delta H^\circ - T\Delta S^\circ$$

(17)

$$\ln K_c = \frac{\Delta S^o}{R} - \frac{\Delta H^o}{RT}$$

(18)

Where T is the absolute temperature (K); R is the gas constant (8.314 $Jmol^{-1}.K^{-1}$). The change in enthalpy and entropy were calculated from the intercept and slope of the plot of T versus ΔG° as presented in Figure 14 while the thermodynamic parameters are presented in Table 3. The negative values of ΔG° indicate spontaneity of each biosorption process, with the order of spontaneity being Zn(II)>Cd(II)>Pd(II). The positive value of ΔH° for the biosorption of the each of the metal ions suggests endothermic nature of the biosorption processes. This is also supported by the increase in the value of biosorption capacity of the biosorbent with rise in temperature. The positive values of ΔS° observed for the biosorption of these metal ions indicate a increase in randomness at the solid/solution interface during their biosorption. The order of decreasing disorder being Zn(II)>Cd(II)>Pb(II). Generally, the change of standard free energy for physiosorption is in the range of −20 to 0 kJ mol^{-1} and for chemisorption varies between −80 and −400 $kJmol^{-1}$ [29, 30]. In the present study, the overall ΔG° has values ranging from −7.5 to −3.5 kJ mol^{-1}. These results correspond to a spontaneous physical adsorption of the metal ions, indicating that this system does not gain energy from external resource [29, 31]. The decrease in ΔG° with increase in temperature indicates more efficient biosorption at higher temperature. This is also supported by the increase in the value of biosorption capacity of the biosorbent with rise in temperature. Furthermore, the magnitude of activation energy (A) gives an idea about the type of adsorption which is mainly diffusion controlled process (not diffusivity of solute through micropore wall surface of a

particle) or chemical reaction processes [32]. Energies of activation, A, below 42 kJ/mol indicate diffusion-controlled processes, and higher values give chemical reaction-based processes. Therefore, energy of activation, A, has been calculated as per the following relation:

$$A = \Delta H^\circ + RT$$

(19)

The values of A at two different temperatures have been tabulated in Table 4. In this study, the activation energy (A) values were less than 42 $kJmol^{-1}$ indicating diffusion-controlled adsorption processes.

4. Conclusion

In this work we have studied the biosorption of Cd(II), Pb(II) and Zn(II) by melon (*Citrillus lanatus*) seed husk under various conditions. The biosorption of each was influenced by each of the parameters investigated. The pH has much effect on the biosorption of these metal ions from aqueous solutions. The rate of the biosorption of these metal ions followed pseudo-second-order kinetics. The sorption isotherms of these metal ions onto the biosorbent are well described by the Freundlich isotherm model. The thermodynamic study shows that the biosorption of each of Cd(II), Pb(II) and Zn(II)was spontaneous in the order Zn(II) >Cd(II) >Pb(II). This study shows that melon seed husk has high potential for treating industrial effluents containing Cd(II), Pb(II) and Zn(II).

References

[1]   G.A. Drasch. (1993). Increase of Cadmium body burden for this century. Science of the Total Environment. 67 75-89.

[2]   X. Zhou., T. Korenaga., T. Takahashi., T. Moriwake and S. Shinoda. (1993). Process monitoring controlling system for the treatment of wastewater containing chromium (VI). Water Resources. 27 1049-1054.

[3]   G. Tiravanti., D. Petruzzelli and R. Passino. (1997). Pretreatment of tannery wastewaters by ion exchange process for Cr(III) removal and recovery. Water Science Technology. 36 197-207.

[4]   N. Kongsricharoern and C. Polprasert. (1996). Chromium removal by a bipolar electrochemical precipitation process. Water Science Technology. 34 109-116.

[5]   A.K. Chakravarti., S.B. Chowdhury., T. Chakrabarty and D.C. Mukherjee. (1995). Liquid membrane multiple emulsion process of Chromium (VI) separation from waste waters. Colloids and Surfaces A. 103 59-71.

[6]   S. Dahbi and M. Azzi. (1999). Removal of hexavalent chromium from wastewaters by bone charcoal. Fresenius Journal of Analytical Chemistry. 363 404-407

[7]   A. Sari., D. Mendi., M. Tuzen and M. Soylak. (2008). Biosorption of Cd(II) and Cr(III) from aqueous solution by moss (*Hylocomium splenders*) biomass: equilibrium, kinetic and thermodynamic studies. Chemical Engineering Journal. 144 1-9

[8]   O.D. Uluozlu, A. Sari, M. Tuzen, M. Soylak. (2008). Biosorption of Pb(II) and Cr(III) from

aqueous solution by lichen (*Parmelinatilaceae*) biomass. Bioresource Technology. 99 2972-2980).

[9] N.A.A. Babarinde., J.O Babalola., A.O. Ogunfowokan and A.C. Onabanjo. (2009). Kinetic, equilibrium and thermodynamic studies of the biosorption of cadmium (II) from solution by *Stereophyllum radiculosum,* Toxicological and Environmental Chemistry. 91(5) 911-922

[10] N.A.A. Babarinde., J.O. Babalola., J. Adegoke., O. Maranzu., T. Ogunbanwo and E. Ogunjinrin. (2012). Kinetic, isothermal and thermodynamic studies of the biosorption of Ni(II) and Cr(III) from aqueous solutions using banana (Musa acuminata) leaf. International Journal of Physical Sciences. 7(9) 1376-1385.

[11] N.A.A. Babarinde., J.O Babalola., J. Adegoke., A. O. Osundeko., S. Olasehinde and A. Omodehin , E. Nurhe. (2013). Biosorption of Ni(II), Cr(III) and Co(II) from solutions using Acalypha hispida leaf: Kinetics, Equilibrium and Thermodynamics, Journal of Chemistry http://dx.doi.org/10.1155//460635)

[12] B. Das and N.K. Mondal. (2011). Calcareous Soil as New adsorbent to remove Lead from Aqueous Solution: Equilibrium, Kinetic and Thermodynamic Study. Universal Journal of Environmental Research and Technology. 1(4) 515-530

[13] G.A. Enoch., F. Rose., T.A. Hermane., S.V. Raymond., C. Ousmane and A. Adam. (2008). Importance and practices of egusi crops (*Citrillus lanatus*). Biotechnology Agronomy, Society and Environment 12(4) 393-40.

[14] O.D. Uluozlu., A. Sari and M. Tuzen. (2010). Biosorption of antimony from aqueous solution by lichen (Physciatribacia). Chemical Engineering Journal. 163 382 -388.

[15] S. Pradhan., S. Singh and L. C. Rai. (2007). Characterization of various functional groups present in the capsule of Microcystis and study of their role in biosorption of Fe, Ni and Cr. Bioresource Technology. 98: 595-60.

[16] B.Y.O. Bueno., M.L. Torem., F. Molina and L.M.S. de Mesquita. (2008). Biosorption of lead(II), chromium (III) and copper (II) by R. opacus: Equilibrium and kinetic studies, Mineral Engineering 21 65-75.

[17] X.F. Sun., S.G. Wang., X.W. Liu., W.X. Gong., N. Bao., B.Y. Gao and H.Y. Zhang. (2008). Biosorption of Malachite Green from aqueous solutions onto aerobic granules: Kinetic and equilibrium studies. Bioresource Technology. 99 3475-3483.

[18] N. Ertugay and Y.K. Bayhan. (2008). Biosorption of Cr(VI) from aqueous solutions by biomass of Agaricusbisporus. Journal of Hazardous Materials. 154 432- 439.

[19] T. Akar., S. Tunali and A. Cabuk. (2007). Study on the characterization of lead(II) biosorption by fungus *Aspergillusparasiticus*. Applied Biochemistry and Biotechnology. 136(3) 389-406.

[20] K. Vijayaraghavan., T.V.N. Padmesh and M. Velan. (2007). Biosorption of Nickel(II) ions onto Sargassum wightii:Application of two parameter and three parameter isotherm models. Journal of Hazardous Materials. 133(1-3) 304-406.

[21] Y. Wu., L. Zhang., C. Gao., X. Ma and R. Han. (2010). Adsorption of copper ions and methylene Blue in a single and Binary System on Wheat straw. Journal Chemical Engineering Data. 54: 3229-3234.

[22] J. Kielland. (1937). Effective diameters of unhydrated and hydrated ions. Journal American Chemical Society. 59 1675-1678.

[23] M. A. Miranda., P. Dhandapani., M. H. Kalavathy and L. R. Miranda. (2010). Chemically activated Ipomoea carnea as an adsorbent for the copper sorpties from synthetic solutions. Adsorption 16(1-2) 73-84.

[24] T.S. Anirudhan., P.G. Radhakrishnan. (2008). Thermodynamics and kinetics of adsorption of Cu(II) from aqueous solutions unto a new cation exchanger derived from tamarind fruit shell. Journal Chemical Thermodynamics. 4(4) 702- 709

[25] Z. Chen, W. Ma and M. Han. (2008). Biosorption of nickel and copper onto treated alga (*Undariapinnarlifida*): Application of isotherm and kinetic models. Journal of Hazardous Materials. 155 (1-2) 327-333.

[26] S. Kundu and A. K. Gupta. (2006). Arsenic adsorption onto iron oxide-coated cement (IOCC): regression analysis of equilibrium data with several isotherm models and their optimization. Chemical Engineering Journal. 122 (1-2) 93-106.

[27] G. de la Rosa., H.E. Reynel-Avila., A. Bonilla-Petriciolet., I. Cano-Rodríguez., C. Velasco-Santos., R. Martínez-Elangovan., L. Pilip and K. Chandraraj. (2008). Biosorption of chromium species by aquatic weeds: Kinetics and mechanism studies. J. of Hazardous Materials.152:100-12.

[28] R. Qu., Y. Zhang., C. Sun., C. Wang., C. Ji., H. Chen and P. Yin. (2010). Adsorption of Hg(II) from an Aqueous Solution by Silica-Gel Supported Diethylenetriamine Prepared via Different Routes: Kinetics, Thermodynamics and Isotherms. Journal Chemical Engineering Data. 55 1496–1504.

[29] V. Vimonses., S. Lei., B. Jin., C.W.K. Chow and C. Saint. (2009). Kinetic study and equilibrium isotherm analysis of Congo red adsorption by clay materials. Chemical Engineering Journal. 148 354–364

[30] T.K. Sen., S. Afroze and H.M. Ang. (2011). Equilibrium, Kinetics and Mechanism of Removal of Methylene Blue from Aqueous Solution by Adsorption onto Pine Cone Biomass of Pinus radiate. Water Air Soil Pollution. 218 499–515

[31] F. Arias and T.K. Sen. (2009). Removal of zinc metal ion (Zn^{2+}) from its aqueous solution by kaolin clay mineral: A kinetic and equilibrium study. Colloids and Surfaces A. 348 100–108.

[32] M.M. Abd EI-Latif., A. M. Ibrahim and M.F. EI-Kady. (2010). Adsorption equilibrium, kinetics and thermodynamics of methylene blue from aqueous solutions using biopolymer oak sawdust composite. Journal American Science. 6(6) 267–283.